Molecular Crystals and Liquid Crystals Incorporating Nonlinear Optics

Publication details, including instructions for authors and subscription information:
http://www.tandfonline.com/loi/gmcl17

Organic Superconductors, $(DMET)_2X$

Isao Ikemoto [a], Koichi Kikuchi [a], Kazuya Saito [a], Kazushi Kanoda [b], Toshihiro Takahashi [b], Keizo Murata [c] & Keiji Kobayashi [d]

[a] Department of Chemistry, Faculty of Science, Tokyo Metropolitan University, Fukazawa, Setagaya-ku, Tokyo, 158, Japan

[b] Department of Physics, Faculty of Science, Gakushuin University, Mejiro, Toshima-ku, Tokyo, 171, Japan

[c] Electrotechnical Laboratory, Umezono, Tsukuba, 305, Japan

[d] Department of Arts and Sciences, The University of Tokyo, Komaba, Meguro-ku, Tokyo, 153, Japan

Version of record first published: 22 Sep 2006.

To cite this article: Isao Ikemoto , Koichi Kikuchi , Kazuya Saito , Kazushi Kanoda , Toshihiro Takahashi , Keizo Murata & Keiji Kobayashi (1990): Organic Superconductors, $(DMET)_2X$, Molecular Crystals and Liquid Crystals Incorporating Nonlinear Optics, 181:1, 185-195

To link to this article: http://dx.doi.org/10.1080/00268949008036003

Mol. Cryst. Liq. Cryst., 1990, vol. 181, pp. 185–195
Reprints available directly from the publisher
Photocopying permitted by license only

Printed in the United States of America

ORGANIC SUPERCONDUCTORS, $(DMET)_2X$

ISAO IKEMOTO, KOICHI KIKUCHI, and KAZUYA SAITO
Department of Chemistry, Faculty of Science, Tokyo Metropolitan University, Fukazawa, Setagaya-ku, Tokyo 158, Japan
KAZUSHI KANODA and TOSHIHIRO TAKAHASHI
Department of Physics, Faculty of Science, Gakushuin University, Mejiro, Toshima-ku, Tokyo 171, Japan
KEIZO MURATA
Electrotechnical Laboratory, Umezono, Tsukuba 305, Japan
KEIJI KOBAYASHI
Department of Arts and Sciences, The University of Tokyo, Komaba, Meguro-ku, Tokyo 153, Japan

Abstract The physical properties of $(DMET)_2X$ are summarized. DMET salts are classified into five groups on the basis of the temperature dependence of electrical conductivities. Among them, seven salts show superconductivities. The crystal structures of typical DMET salts within each group are described. These salts have the crystal structures characteristic to each group which are reflected in their physical properties. The phase diagram of the first DMET superconductor, $(DMET)_2Au(CN)_2$ is also presented.

INTRODUCTION

Since the first discovery of superconductivity in organic material, a number of organic superconductors have been found in TMTSF and BEDT-TTF families. However, there are many differences in the properties between two families. Recently we have discovered seven organic superconductors in the family of the unsymmetrical donor DMET.[1-5] These new superconductors are the first ones based on an unsymmetrical molecule. They are also important for understanding the organic superconductors systematically, because DMET has the half structures of TMTSF and BEDT-TTF (Fig. 1) and DMET salts seem to link the TMTSF and

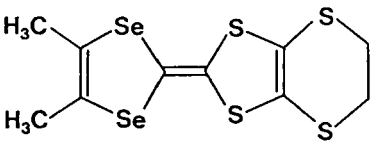

FIGURE 1. Molecule of DMET.

BEDT-TTF families together. Indeed the investigation of the temperature dependence of the resistivities revealed that DMET salts can be classified into five groups and some groups are similar to TMTSF salts and some BEDT-TTF salts.[6,7] In this paper, we summarize the crystal structures and the physical properties of DMET salts. We also present the phase diagram of the the first DMET superconductor, $(DMET)_2Au(CN)_2$.

PHYSICAL PROPERTIES OF DMET SALTS

The temperature dependence of resistivity of typical DMET salts are shown in Fig. 2.[7] The salts are classified into five groups. The salts with octahedral anions are semiconductors below, at least, room temperature. The salts with tetrahedral anions show a broad metal-insulator transition.

DMET salts with linear anions show three different types of temperature dependence of resistivity. $(DMET)_2Au(CN)_2$ exhibits a

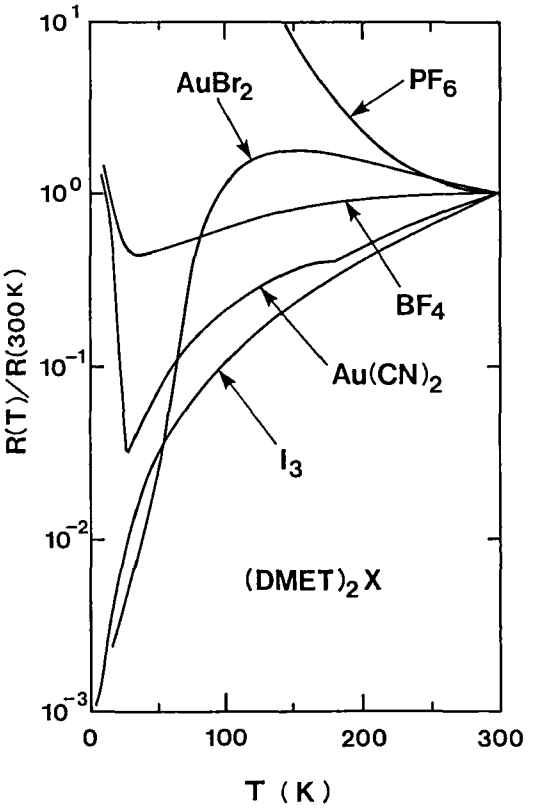

FIGURE 2. Temperature dependence of the resistivity of $(DMET)_2X$.

metal-insulator transition at 28 K at ambient pressure, and a superconducting transition around 1 K under pressure.[1] The electrical property of $Au(CN)_2$ salt is similar to those of TMTSF salts. The property of $Au(CN)_2$ salt is discussed later in detail. AuI_2 and $AuCl_2$ salts show the similar temperature dependence to $Au(CN)_2$ salt at ambient pressure and also have a superconducting phase.[4]

$(DMET)_2I_3$ shows a superconducting transition at ambient pressure at 0.5 K, above which the resistivity is metallic.[3] This temperature dependence is similar to those of β-(BEDT-TTF)$_2$X. $(DMET)_2X$ (X= IBr_2, I_2Br, SCN and $AuBr_2$) also show no resistance upturn, but only IBr_2 undergoes a superconducting transition.

Rhombus-like $(DMET)_2AuBr_2$ shows another type of temperature dependence of resistivity.[5] It showa a broad resistance maximum at 150 K or 180 K. Such a resistance maximum is also observed in -(BEDT-TTF)$_2$Cu(NCS)$_2$. The crystal which has a resistance maximum at 150 K undergoes a superconducting transition at 1.9 K at ambient pressure. The crystal which has a maximum at 180 K exhibits superconductivity only under some pressure.

We also investigated the magnetic properties of typical DMET salts through ESR measurements. The spin susceptibility χ and the linewidth ΔH of typical DMET salts are summarized in Fig. 3.[8] DMET salts have similar spin susceptibilities except rhombus-like $AuBr_2$ salt, but the linewidths are different. The linewidth becomes wider in the order of the PF_6, BF_4, $Au(CN)_2$, I_3, and $AuBr_2$ salts. If we assume that the Elliott mechanism is responsible for the ESR linewidth, the dimensionality may become larger in the same order. This order is in accord with the expextation from the difference of the temperature dependence of resistivity.

For PF_6, BF_4, and $Au(CN)_2$ salts, the susceptibility decreases abruptly below 20-25 K, indicating some magnetic transition. A clear line broadening below 20 K in BF_4 salt is indicative of an antiferromagnetic transition. $Au(CN)_2$ salt shows no line broadening although a kink is observed in the transition region. The ^1H NMR studies on this salt have shown clear antiferromagnetic nature of the transition.[9] The detail is discussed later. In PF_6 salt, the ESR line broadening is very small and starts far below the transition in the susceptibility. Thus we have no confidence of antiferromagnetic nature

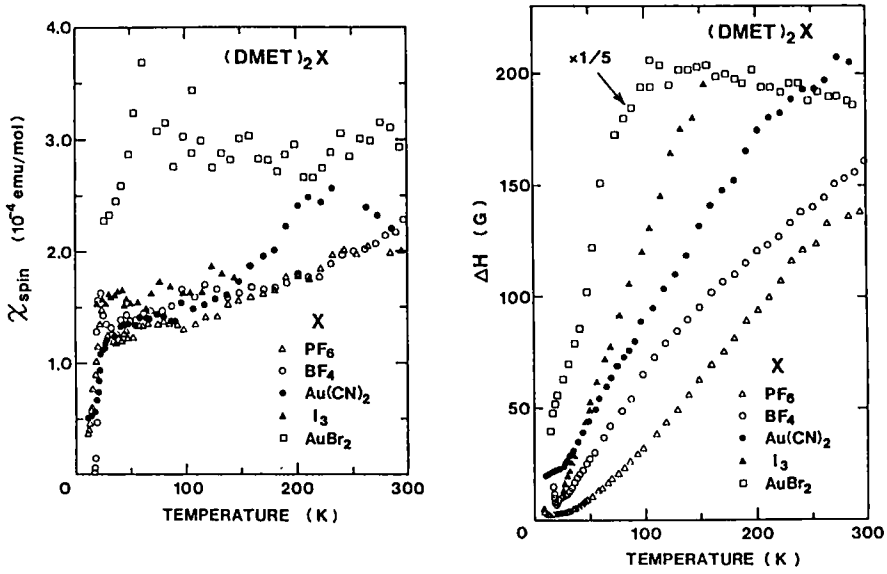

FIGURE 3. Temperature dependence of the spin susceptibility χ_{spin} and the linewidth ΔH of ESR absorption of $(DMET)_2X$.

at present; a spin-Peierls transition is also not ruled out. We have found that SbF_6 and ClO_4 salts undergo antiferromagnetic transition at 20 K. Therefore many DMET salts have antiferromagnetic ground states with almost the same transition temperatures.

$(DMET)_2AuBr_2$ is exceptional among DMET salts.[10] χ is larger than any other DMET salts. The magnitude and the temperature dependence of ΔH are also anomalous. At room temperature, ΔH is 930 G and this value is extraordinarily large among organic conductors. As temperature decreases, ΔH increases gradually and shows a maximum

TABLE 1. Properties of $(DMET)_2X$ superconductors.

X	σ_{rt} / (S cm^{-1})	T_{sc} / K	P_c / kbar
$Au(CN)_2$	220	0.80*	1.5
AuI_2	300	0.55*	5.0
$AuCl_2$	230	0.83	0
I_3	160	0.47	0
IBr_2	210	0.58	0
$AuBr_2$	0.77	1.9	0
$AuBr_2$	13	1.0**	

*Value at 5.0 kbar. **Value at 1.5 kbar.

around 1 K, then decreases rapidly at lower temperature. Such an anomalous temperature dependence corresponds well to that of the resistivity. These ESR results support that the electronic state of this salt actually has some anomaly around 150 K.

In DMET family, seven salts have found to show superconductivity so far. Table 1 is the summary of the physical properties of DMET superconductors.

CRYSTAL STRUCTURES OF DMET SALTS

The crystal structure of $(DMET)_2PF_6$ is shown in Fig. 4.[11,12] A columnar structure is observed as in $(TMTSF)_2X$ salts. The normal to the DMET molecular plane is largely tilted from the stacking axis and some dimerization is observed, which may be related to the semiconductive behavior of the electrical resistivity of this salt. The crystal structure of $(DMET)_2BF_4$ is shown in Fig. 5.[12] This salt has columns of DMET not only along the b axis, but also along the c axis and the columns are almost perpendicular to each other. This structure is very peculiar though the similar structure has been reported in (DMET-TTF)$_2ClO_4$. The stack along the b axis is similar to one in $(DMET)_2PF_6$ salt, but little dimerization is observed in the column in contrast to $(DMET)_2PF_6$. The stack along the c axis is similar to ones observed in

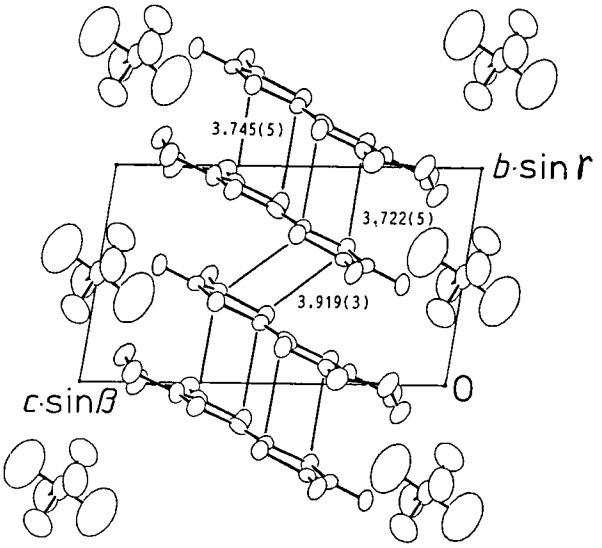

FIGURE 4. Crystal structure of $(DMET)_2PF_6$.

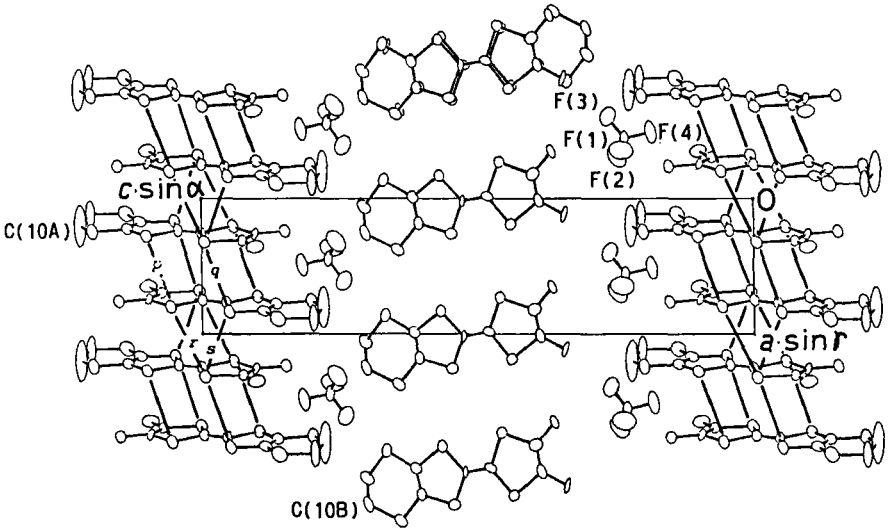

FIGURE 5. Crystal structure of $(DMET)_2BF_4$.

most of $(TMTSF)_2X$ salt, that is, the stacking axis is almost normal to the DMET molecular plane in this stack. Little dimerization is also observed in this stack. Little dimerization is consistent with metallic behavior of this salt. The other structural character of $(DMET)_2BF_4$ salt is the weak interstack interaction between both types of column, but two dimensional character of electrical property is expected because of the presence of two types of column along two directions.

The crystal structure of $(DMET)_2Au(CN)_2$ is shown in Fig. 6.[13] The stack of DMET along the b axis is similar to one in $(DMET)_2PF_6$. Little dimerization is observed in the column. As three shorter contacts are observed between columns than the sum of van der Waals radii, this salt has some two-dimensional character.

The structure of I_3 salt is very similar to that of $Au(CN)_2$ salt, but their electrical properties are different from each other. $(DMET)_2Au(CN)_2$ salts is similar to TMTSF salts and $(DMET)_2I_3$ salt is similar to β-BEDT-TTF salts. The difference in properties between TMTSF and BEDT-TTF salts has generally thought to be caused by difference in dimensionality. TMTSF salts have less two-dimensional character than BEDT-TTF salts, so they have SDW and superconducting phases. On the other hand, the electronic systems of BEDT-TTF salts are

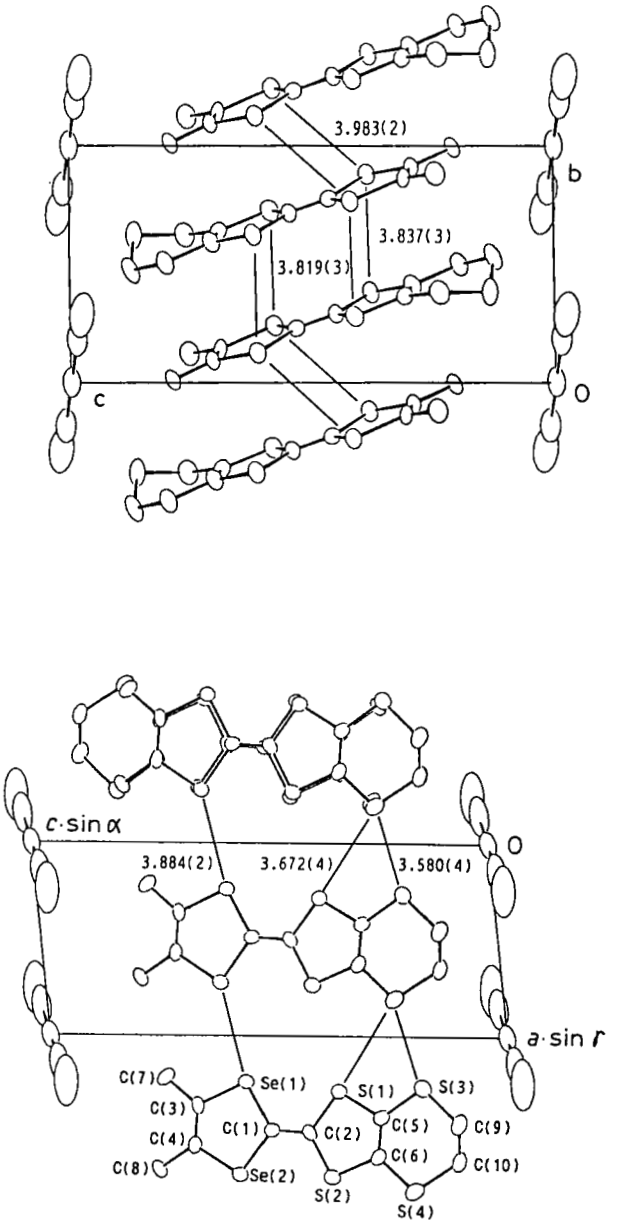

FIGURE 6. Crystal structure of $(DMET)_2Au(CN)_2$.

TABLE 2. Comparison of distances of short intercolumnar atomic contact in DMET superconductors.

Salt	Se-Se / Å	S-S / Å	S-S / Å
$(DMET)_2Au(CN)_2$	3.884	3.580	3.672
$(DMET)_2AuI_2$	3.832	3.552	3.611
$(DMET)_2I_3$	3.784	3.504	3.604
$(DMET)_2IBr_2$	3.774	3.494	3.588

simple, being metallic and superconducting. Table 2 shows the distances of short interstack contacts of DMET superconductors which have the structure similar to that of $Au(CN)_2$ salt. The distances in I_3 and IBr_2 are shorter than the corresponding distances in $Au(CN)_2$ and AuI_2 salts. This suggests that $Au(CN)_2$ and AuI_2 salts have less two-dimensionality than I_3 and IBr_2 salts. This fact is consistent with their electrical properties. That is, less two-dimensional $Au(CN)_2$ and AuI_2 salts have SDW and superconducting phases and more two-dimensional I_3 and IBr_2 salts have simple electronic system.

Figure 7 shows the crystal structure of rhombus-like $AuBr_2$ salt.[5] The structure is not columnar in contrast to other DMET salts. It consists of sheets of dimers of DMET molecules and $AuBr_2$ anions, so this salt is two-dimensional. This structure is very similar to that of κ-$(BEDT\text{-}TTF)_2Cu(NCS)_2$. This is consistent with their similarity in electrical properties.

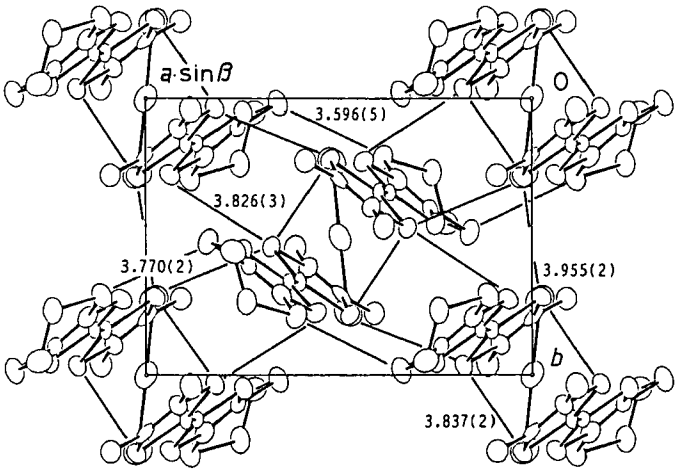

FIGURE 7. Crystal structure of $(DMET)_2AuBr_2$.

PHASE DIAGRAM OF (DMET)$_2$Au(CN)$_2$

Figure 8 shows the pressure-temperature phase diagram of (DMET)$_2$Au(CN)$_2$ which is determined through the electrical resistivity measurements.[14] At ambient pressure, (DMET)$_2$Au(CN)$_2$ is metallic down to 28 K, below which the resistance turns to increase as shown in Fig. 2. The increase of resistivity at low temperature is due to the spin density wave (SDW) state, which is confirmed with the ^{1}H NMR study.

Figure 9 shows the temperature dependence of the ^{1}H NMR linewidth ΔH and the invrerse of the spin-lattice relaxation time, T_1^{-1}.[9] ΔH keeps a constant value of 8 G down to 20 K and starts to increase toward 12.5 G. Therefore the excess broadening at low temperatures can be estimated as 10 G. Since the proton has no quadrupole moment, the broadening should be a clear evidence of the onset of the excess local field due to the transition, That is, the broadening is the evidence of the magnetic transition. The same phenomena were observed below the SDW transition in (TMTSF)$_2$X and (TMTTF)$_2$X. The excess local field is

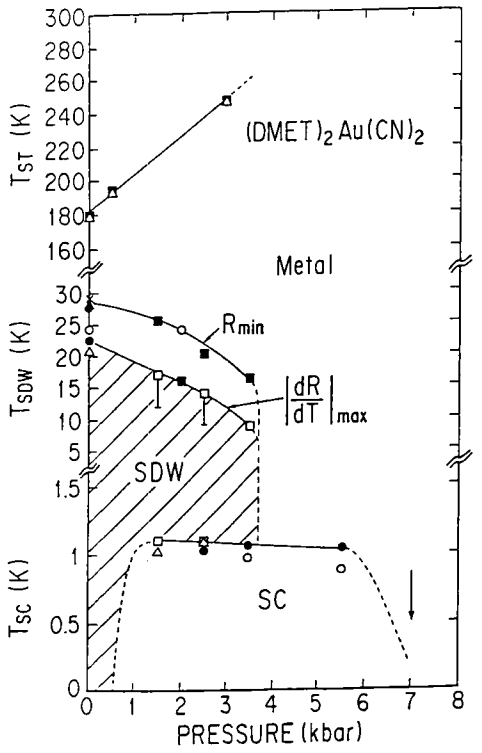

FIGURE 8. *T-P* phase diagram of (DMET)$_2$Au(CN)$_2$. The boundary between the SDW and the normal phases is plotted as the points of the resistance minimum.

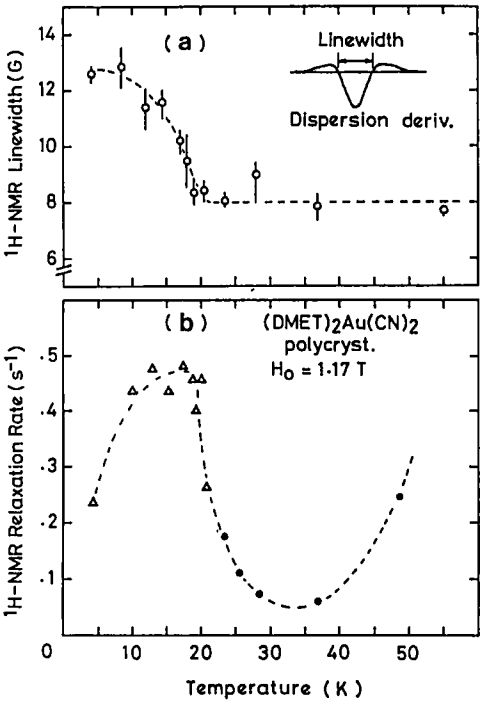

FIGURE 9. ^{1}H NMR linewidth and the spin-lattice relaxation rate of (DMET)$_2$Au(CN)$_2$.

almost the same in magnitude as those in the previous SDW's. Then the SDW amplitude in (DMET)$_2$Au(CN)$_2$ should be the order of 0.1 μ_B per molecule.

At ambient pressure, a sharp dip is also observed in the temperature dependence of resistivity at 180 K, suggesting another phase transition. This transition was detected in the measurement of thermoelectric power and heat capacity. The heat capacity measurement suggested that the transition is of higher order.[15,16]

With increasing pressure, SDW is suppressed, vanishing above 3.5 kbar, as shown in Fig. 8. The superconductivity is present between 1.5 kbar and 5.5 kbar. The pressure region in which both SDW and superconductivity are observed is as wide as 4 kbar, which is much wider than (TMTSF)$_2$X. The temperature of the dip in resistivity increase with increasing temperature, and the dip becomes weak and disappears above 3.5 kbar. The pressure region of the SDW and the dip at high temperature coincided.

ACKNOWLEDGMENT

This work was supported in part by Grant-in-Aid for Specially Promoted Research (No. 63060004) from the Ministry of Education, Science and Culture.

REFERENCES

1. K. Kikuchi, M. Kikuchi, T. Namiki, K. Saito, I. Ikemoto, K. Murata, T. Ishiguro, and K. Kobayashi, *Chem. Lett.*, 931(1987).
2. K. Kikuchi, K. Murata, Y. Honda, T. Namiki, K. Saito, K. Kobayashi, T. Ishiguro, and I. Ikemoto, *J. Phys. Soc. Jpn.*, **56**, 2627(1987).
3. K. Kikuchi, K. Murata, Y. Honda, T. Namiki, K. Saito, K. Kobayashi, T. Ishiguro, and I. Ikemoto, *J. Phys. Soc. Jpn.*, **56**, 3436(1987).
4. K. Kikuchi, K. Murata, Y. Honda, T. Namiki, K. Saito, K. Kobayashi, T. Ishiguro, and I. Ikemoto, *J. Phys. Soc. Jpn.*, **56**, 4241(1987).
5. K. Kikuchi, Y. Honda, Y. Ishikawa, K. Saito, I. Ikemoto, K. Murata, H. Anzai, T. Ishiguro, and K. Kobayashi, *Solid State Commun.*, **66**, 405(1988).
6. K. Murata, K. Kikuchi, T. Takahashi, K. Kobayashi, Y. Honda, K. Saito, K. Kanoda, T. Tokiwa, H. Anzai, T. Ishiguro, and I. Ikemoto, *J. Mol. Electron.*, **4**, 173(1988).
7. K. Kikuchi, K. Saito, I. Ikemoto, K. Murata, T. Ishiguro, and K. Kobayashi, *Synth. Metals*, **27**, B269(1988).
8. K. Kanoda, T. Takahashi, K. Kikuchi, K. Saito, I. Ikemoto, and K. Kobayashi, *Phys. Rev.*, **B39**, 3996(1989).
9. K. Kanoda, T. Takahashi, T. Tokiwa, K. Kikuchi, K. Saito, I. Ikemoto, and K. Kobayashi, *Phys. Rev.*, **B38**, 39(1988).
10. K. Kanoda, T. Takahashi, K. Kikuchi, K. Saito, Y. Honda, I. Ikemoto, K. Kobayashi, K. Murata and A. Anzai, *Solid State Commun.*, **69**, 415(1989).
11. K. Kikuchi, I. Ikemoto, and K. Kobayashi, *Synth. Metals*, **19**, 551(1987).
12. K. Kikuchi, Y. Ishikawa, K. Saito, I. Ikemoto and K. Kobayashi, *Synth. Metals*, **27**, B391(1988).
13. K. Kikuchi, Y. Ishikawa, K. Saito, I. Ikemoto and K. Kobayashi, *Acta Cryst.*, **C44**, 466(1988).
14. Y. Honda, K. Murata, K. Kikuchi, K. Saito, I. Ikemoto, and K. Kobayashi, *Solid State Commun.*, **71**, 1087(1989).
15. K. Saito, K. Kamio, K. Kikuchi, K. Kobayashi, and I. Ikemoto, *J. Phys.:Condensed Matt.*, in press.
16. K. Saito, K. Kamio, Y. Honda, K. Kikuchi, K. Kobayashi, and I. Ikemoto, *J. Phys. Soc. Jpn.*, **58**(11), (1989).